2

NASA CR-122509

Final Report

for

"Energetic Radiations from Solar Flares"

Experiment

(OGO-5)

March, 1968 - August, 1971

Contract No. NAS 5-9094

Principal Investigator: K. A. Anderson

42

Space Science Laboratory Series 13, Issue 50

Space Sciences Laboratory Series 13, Issue 50

FINAL REPORT

FOR

"ENERGETIC RADIATIONS FROM SOLAR FLARES"

EXPERIMENT

(OGO-5)

(March, 1968 - August, 1971)

Contract No. NAS 5-9094

Prepared by

Space Sciences Laboratory
University of California
Berkeley, California 94720

Principal Investigator: K. A. Anderson

for

Goddard Space Flight Center
Greenbelt, Maryland

CONTENTS

LIST OF ILLUSTRATIONS

LIST OF TABLES

ABSTRACT

This report describes the University of California (Berkeley) experiment "Energetic Radiations from Solar Flares" aboard the OGO-5 satellite. The experiment was designed to measure energetic X-rays, electrons, protons and α-particles from solar flares. This report consists of a brief statement of the objectives of the experiment followed by a description of the instrumentation including the detector characteristics and associated electronics. The data handling system is then described and the operational history of the experiment is discussed. This is followed by a description of the format of the magnetic data tapes to be supplied to the National Space Science Data Center and a summary of the major computer processing programs.

The measurements made with this experiment within the first year of its operation have led to several basic results regarding the role of non-thermal electrons in the physics of solar flares. These results are described in the papers listed in the bibliography given at the end of this report. The data from this experiment is still being analyzed in collaboration with experimentors having detectors aboard other spacecraft as well as those making ground based measurements.

I. OBJECTIVE

The objective of the experiment is to study the time variation of the spectrum of energetic X-rays, protons, α-particles and electrons emitted by the sun in association with solar flares. In order to make meaningful measurements, it is essential that during most of the orbit the satellite be located outside the region of the earth's magnetospheric radiation. Also a time resolution $\lesssim 1$ sec is essential for the solar X-ray measurements. Both of these requirements were well satisfied by the OGO-5 spacecraft.

II. INSTRUMENTATION

The experiment consists of the following three parts:

(1) A NaI(Tl) scintillation counter which measures solar X-rays from 10 keV-200 keV in eight energy channels.

(2) A solid state detector telescope which measures protons ≥ 7 MeV and α-particles ≥ 28 MeV in six energy channels each.

(3) A magnetic spectrometer which measures electrons in the range 22-27 keV and 50-90 keV.

All the detectors are located on a solar panel (Module SOEP-1) of the OGO-5 spacecraft so that they continuously look in the solar direction. The digital data handling system occupies the Module 18 location in the main body of the spacecraft. The characteristics of the individual detectors, energy channels, data averaging time and time between data readout are summarized in Table I. Details regarding the arrangement of the detectors and their response characteristics are given below. A block diagram of the associated electronics is shown in Figure 1.

Table 1. OGO-5 DETECTORS

Detector	Radiation	Energy Channel	Geometry Factor	Data Averaging Time*	Time Between Read-out*
NaI(Tl) scintillator	X-rays	9.6-19.2 keV 19.2-32 keV 32-48 keV 48-64 keV 64-80 keV 80-104 keV 104-128 keV >128 keV	9.5 cm^2 for parallel beam, ~15 cm^2 sr for omni-directional radiation (for all channels)	1.152 sec for all channels	2.304 sec for all channels
Solid state detector telescope	Protons	7-20 meV 20-45 meV 45-80 meV 80-130 meV 130-200 meV >200 meV	3.08 cm^2sr 1.99 cm^2sr 1.17 cm^2sr 0.605 cm^2sr 0.273 cm^2sr 0.011 cm^2sr	147 sec 9.216 sec 9.216 sec 9.216 sec 9.216 sec 9.216 sec	147 sec 9.216 sec 9.216 sec 9.216 sec 9.216 sec 9.216 sec
	α-particle	28-80 meV 80-180 meV 180-320 meV 320-520 meV 520-800 meV >800 meV	3.08 cm^2sr 1.99 cm^2sr 1.17 cm^2sr 0.605 cm^2sr 0.273 cm^2sr 0.110 cm^2sr	147 sec 9.216 sec 9.216 sec 9.216 sec 9.216 sec 9.216 sec	147 sec 9.216 sec 9.216 sec 9.216 sec 9.216 sec 9.216 sec
Magnetic Spectro-meter	Electrons	22-27 keV 50-90 keV	0.1 cm^2sr 0.2 cm^2sr	147 sec 147 sec	147 sec 147 sec

* The data averaging time and the time between read-out correspond to 1 kilobit/sec telemetry rate.

DETECTOR SYSTEM BLOCK DIAGRAM

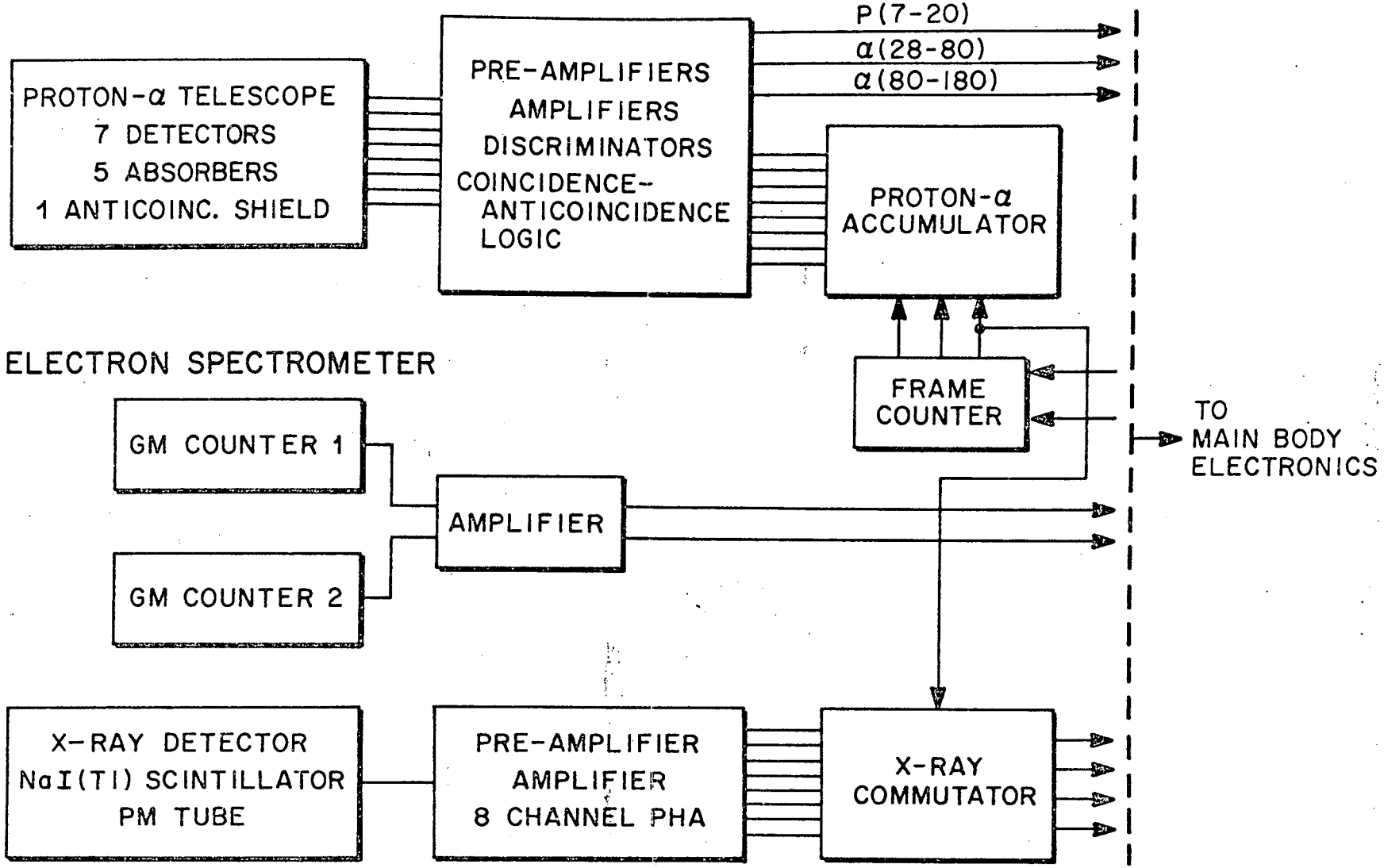

Figure 1

A. Solar X-ray Experiment

The X-ray detector for the OGO-5 experiment consists of a NaI(Tl) crystal 0.5 cm thick and 9.5 cm^2 in area, with a berylium window of thickness 0.051 cm. The scintillator is a cleaved crystal assembly similar to Harshaw Chemical No. 5.5 HD 197 K-x with the exception of a 20 mil berylium front window and a pyrex rear window. The crystal is coupled to an RCA C 70114 F photomultiplier tube (PMT) operated at 1200 volts. The combination yielded a resolution of ~60% FWHM at 29 KeV.

The charge pulses from the PMT are integrated and amplified with an RC time constant of 1.25 μ sec. This time constant is a compromise between charge collection efficiency and pulse pile-up at high pulse rates. The pulse height analyzer (PHA) consists of eight level discrimination followed by eight coincidence-anticoincidence logic units to yield seven differential energy windows and one integral edge. The energy levels are as follows:

Channel No.	Energy Range (keV)
1	9.6 to 19.2
2	19.2 to 32
3	32 to 48
4	48 to 64
5	64 to 80
6	80 to 104
7	104 to 128
8	> 128

The outputs of the eight channel PHA are commutated, four channels at a time, and routed via the spacecraft harness to the data handling system in the main body of the spacecraft.

Before launch, the detector was calibrated with I^{129} and Co^{60} sources. The counting rates of the eight pulse height channels were consistent with the energy windows assigned to them.

The response of the experiment to a parallel beam of photons incident normally on the detector has been computed in the following manner. Consider a beam of monoenergetic photons of energy E(keV) and flux one photon cm^{-2} sec^{-1} incident on the area A (cm^2) of the detector. The number of photons absorbed in the scintillator is given by

$$n_o(E) = Ae^{-\mu_B(E)t_B}\left(1 - e^{-\mu_N(E)t_N}\right) \text{ photons sec}^{-1} \quad ---- \quad (1)$$

where t_B and t_N are respectively the thickness (g cm^{-2}) of the Be window and NaI (Tl) scintillator, μ_B is the photon attenuation coefficient (cm^2 g^{-1}) of Be and μ_N is the photon absorption coefficient (cm^2 g^{-1}) of NaI.

The pulse height distribution at the output of the phototube is given by

$$\frac{dN}{dE'}(E,E') = \frac{1}{\sqrt{2\pi}} \frac{n_o(E)}{\sigma(E)} e^{-\frac{(E-E')^2}{2\sigma^2(E)}} \text{ pulses sec}^{-1} \text{ keV}^{-1} \quad ---- \quad (2)$$

where E' is the pulse height in keV and $\sigma(E)$ is the standard deviation of the pulse height distribution. For the OGO-5 detector it is given

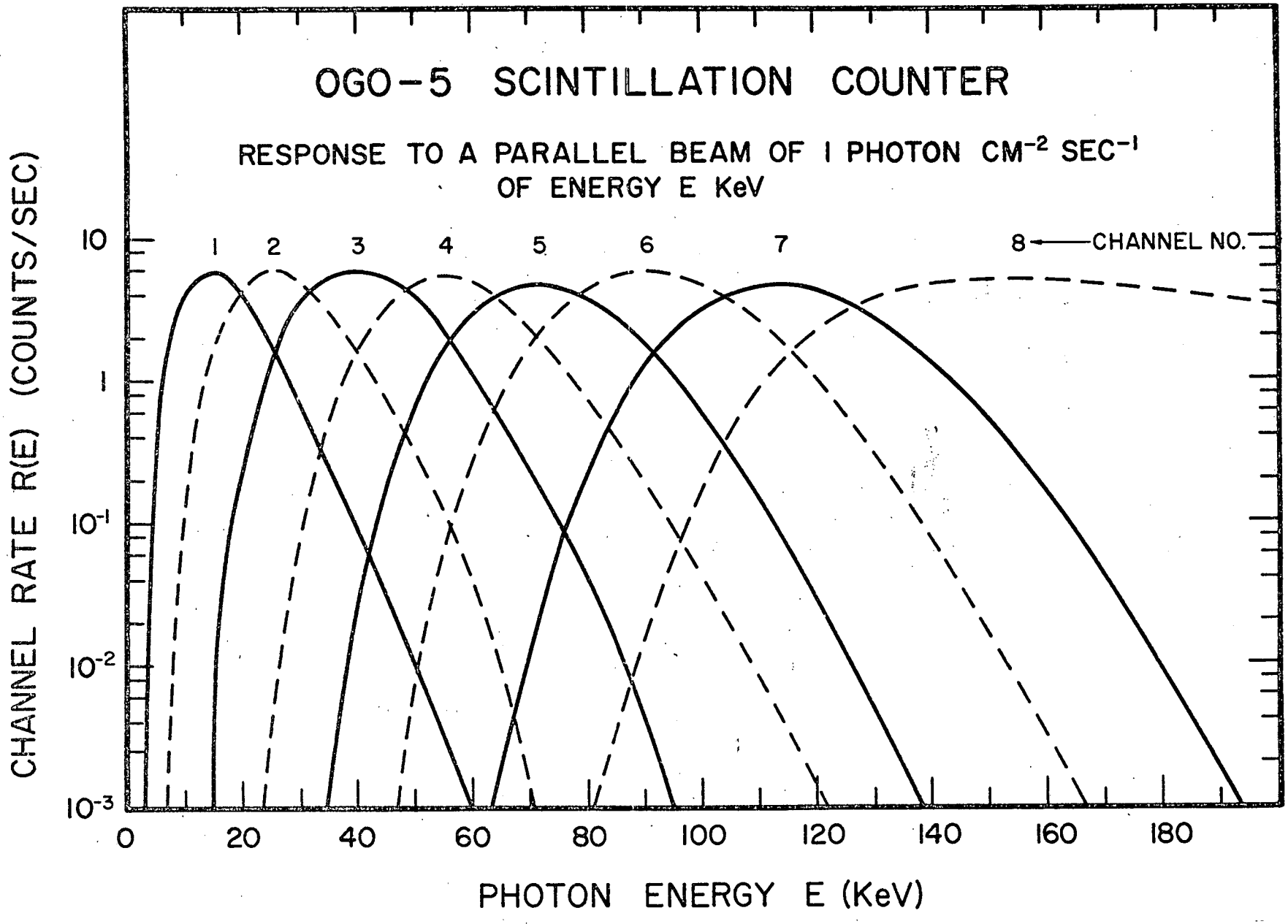
OGO-5 SCINTILLATION COUNTER
RESPONSE TO A PARALLEL BEAM OF 1 PHOTON CM^{-2} SEC^{-1}
OF ENERGY E KeV
CHANNEL RATE R(E) (COUNTS/SEC)
10
1
10^{-1}
10^{-2}
10^{-3}
1
2
3
4
5
6
7
8 — CHANNEL NO.
0
20
40
60
80
100
120
140
160
180
PHOTON ENERGY E (KeV)

Figure 2

by

$$\sigma(E) \approx 1.37\ E^{\frac{1}{2}}\ \text{keV} \qquad ----- \qquad (3)$$

Let the pulse height channels be designated by i = 1,2,...8, the lower edges of the channels being $E_i' = E_1', E_2', \ldots E_8'$ keV respectively. Also let $E_9' = \infty$. Then the counting rate of the ith channel $(E_i' - E_{i+1}')$ due to a monoenergetic beam of one photon $cm^{-2}\ sec^{-1}$ is given by

$$N_{i,\ i+1}(E) \approx \frac{1}{\sqrt{2\pi}} \frac{n_0(E)}{\sigma(E)} \int_{E_i'}^{E_{i+1}'} e^{\frac{(E - E')^2}{2\sigma^2(E)}}\ dE' \text{ counts sec}^{-1} \qquad ----- \qquad (4)$$

The response of the eight energy channels computed in this manner is shown in Figure 2.

For an arbitrary photon spectrum $\frac{dJ}{dE}$ photons $cm^{-2}\ sec^{-1}\ keV^{-1}$, the response of the ith channel is given by

$$n_{i,\ i+1} = \int_{\Theta}^{\infty} N_{i,\ i+1}(E)\ \frac{dJ}{dE}\ dE \text{ counts sec}^{-1} \qquad ----- \qquad (5)$$

For a power law spectrum of the form

$$\frac{dJ}{dE} = KE^{-\gamma} \text{ photons cm}^{-2}\ \text{sec}^{-1}\ \text{keV}^{-1} \qquad ----- \qquad (6)$$

the response of the 7 differential energy channels is shown in Figure 3.

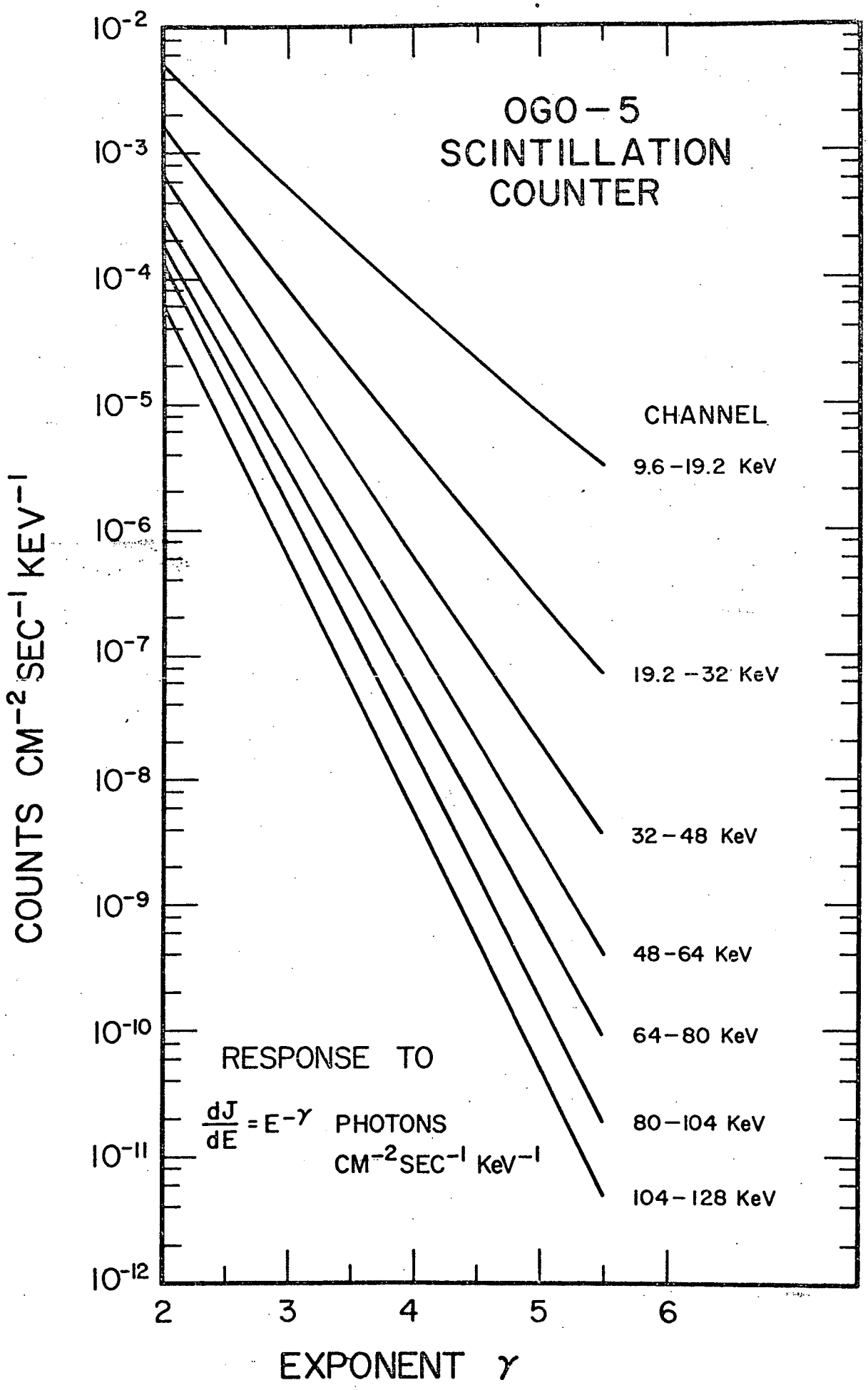
OGO-5
SCINTILLATION
COUNTER
CHANNEL
9.6-19.2 KeV
19.2-32 KeV
32-48 KeV
48-64 KeV
64-80 KeV
80-104 KeV
104-128 KeV
RESPONSE TO
dJ/dE = E^-γ PHOTONS
CM^-2 SEC^-1 KeV^-1
COUNTS CM^-2 SEC^-1 KEV^-1
EXPONENT γ
10^-2
10^-3
10^-4
10^-5
10^-6
10^-7
10^-8
10^-9
10^-10
10^-11
10^-12
2
3
4
5
6

Figure 3

Here the response is expressed in terms of

$$\frac{n_{i,i+1}}{A(E'_{i+1} - E'_i)} \text{ counts cm}^{-2} \text{ sec}^{-1} \text{ keV}^{-1} .$$

The maximum counting rate observable in an individual energy channel is about 28,000 count/sec which is the saturation level determined by the response time of the pulse height discriminator and counting circuits of the experiment. The overall dynamic range of the experiment is such that the solar flares which can be observed without a saturation of the experiment have an optical importance $\lesssim 1$.

When the OGO-5 detector is exposed to a very steep X-ray spectrum the observed counting rates show an apparent hardening of the spectrum with the increase in the incident X-ray intensity even if the spectral shape of the incident radiation remains unchanged. The effect is attributed to pulse pile-up. It limits the possible spectral measurements with the OGO-5 experiment to an incident X-ray spectrum with the spectral exponent $\gamma \lesssim 5$ in case of a power law spectrum ($\sim E^{-\gamma}$ photons cm^{-2} sec^{-1} keV^{-1}) or "thermal" spectra with temperatures $> 3 \times 10^7$ °K and such that the total counting rate of the detector is $< 10^4$ counts/sec.

When the solar activity is low and the OGO-5 satellite is outside the earth's magnetosphere, the counting rates in the different energy channels are essentially those expected from the cosmic X-ray background in the energy range 10 to 128 keV. This can be seen from Figure 4 where the OGO-5 background counting rates in the seven differential energy channels are compared with those observed by Hudson et al. (*Ap. J.* 157, 389, 1969) with a cosmic X-ray experiment aboard the OSO-III satellite when their detector was not looking at the sun. In

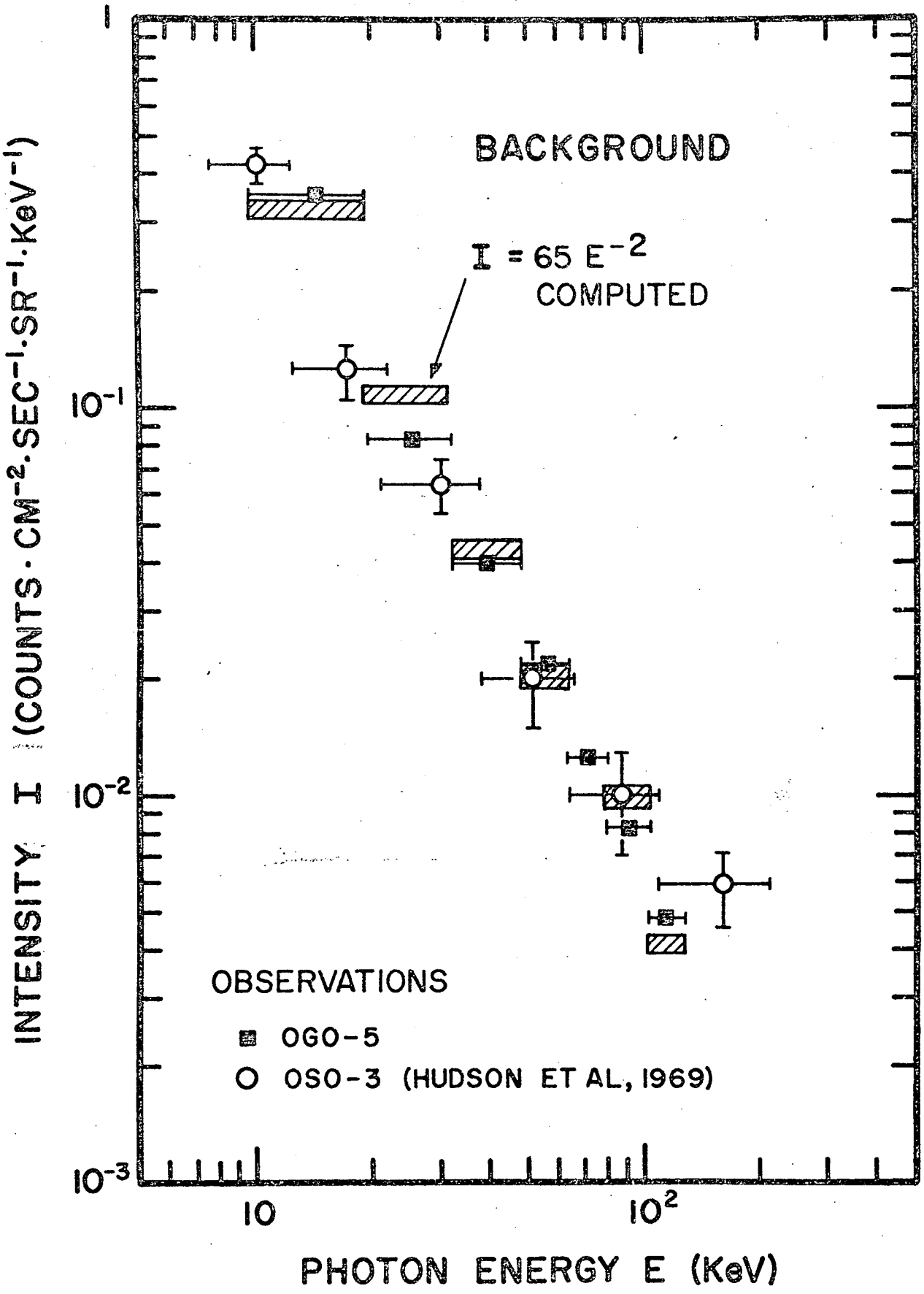
BACKGROUND
I = 65 E⁻²
COMPUTED
OBSERVATIONS
OGO-5
OSO-3 (HUDSON ET AL, 1969)
INTENSITY I (COUNTS · CM⁻² · SEC⁻¹ · SR⁻¹ · KeV⁻¹)
PHOTON ENERGY E (KeV)
1
10⁻¹
10⁻²
10⁻³
10
10²

Figure 4

order to make a valid comparison the intensity I is determined in a manner equivalent to that used by Hudson et al. That is, if R_{ij} counts/sec be the background counting rate of a channel having E_i keV and E_j keV as its lower and upper edges respectively, then

$$I(E) = \frac{R_{ij}}{G(E_j - E_i)} \text{ counts cm}^{-2} \text{ sec}^{-1} \text{ sr}^{-1} \text{ keV}^{-1} \quad (7)$$

where $E = \frac{1}{2}(E_i + E_j)$ keV and G = geometry factor of the detector (cm^2 sr).

From Figure 4 it can be seen that the agreement between the OGO-5 and OSO-III measurements is excellent. This indicates that even though the OGO-5 detector is looking continuously at the sun, the background in the 10 to 128 keV channels observed at times of low solar activity is essentially due to the cosmic X-rays. Further it shows that the pre-launch calibration of the detector remained essentially unchanged during the launch of the OGO-5 spacecraft.

In addition to X-rays, the detector is also sensitive to particles penetrating the berylium window, viz. protons >8 MeV and electrons $\gtrsim$300 keV. Response to electrons < 300 keV is primarily through bremsstrahlung produced in the window. Consequently the detector background is considerably higher during solar cosmic ray events and when the OGO-5 satellite is sampling magnetospheric radiation. Under those circumstances the background is sometimes so large that the experiment is unable to make meaningful measurements of solar X-ray bursts.

B. Proton and α-Particle Telescope

A range telescope consisting of seven solid state detectors (D_1, D_2, . . . D_7), five tungsten absorbers (A_1, A_2, . . . A_5) and an anti-

TABLE 2

SOLID STATE DETECTORS				TUNGSTEN ABSORBERS	
DETECTOR NO.	DETECTOR TYPE	SENSITIVE DEPTH (μ)	SENSITIVE DIAMETER (mm.)	ABSORBER NO.	THICKNESS (mm.)
D_1	PIN	200	12.8	A_1	0.406
D_2	PIN	200	15.5	A_2	1.499
D_3	PIN	200	15.5	A_3	3.607
D_4	PIN	200	15.5	A_4	7.645
D_5	PIN	200	15.5	A_5	14.859
D_6	PIN	200	15.5		
D_7	Li drift PIN	~ 400	15.5		

PROTON-α TELESCOPE (OGO-5)
(ANTI-COINCIDENCE SCINTILLATOR NOT SHOWN)

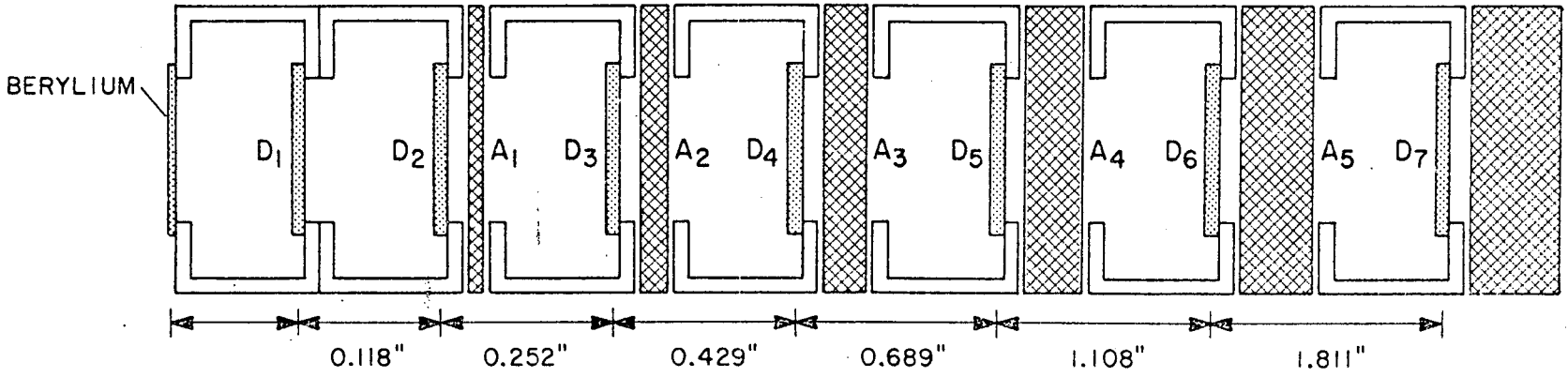

D - SOLID STATE DETECTOR
A - TUNGSTEN ABSORBER

Figure 5

coincidence scintillator shield is used for proton and α-particle measurements. Details of the detector assembly are given in Figure 5 and Table 2. An absorber equivalent to 150μ of silicon is placed at the front of the telescope to protect D1 from low energy radiation damage and from light leaks. A thick absorber at the rear of the telescope performs the same function for D7.

The energy spectrum is divided into the segments shown in Table 3 by defining the particle range with absorbers and coincidence-anticoincidence logic. Because most of the range determination is provided by the passive absorber, the energy separation (except for minimum ionizing protons) can tolerate ±20% variations in discrimination levels and even larger variations in energy resolution.

The field of view, defined by the geometry of the telescope assembly and by the anticoincidence shield, varies with different energy intervals as shown in Table 4.

Basically the particle range is determined by requiring a pulse output from the detector in front of a given absorber and no pulse output from the detector immediately behind that absorber. Protons and alphas are distinguished from each other by their rate of energy loss (dE/dx) in the front detector (D_1). The average energy losses in D_1 for particles stopping in various detectors are shown in Table 4. Thirteen discriminators with the thresholds shown in Table 5 are required for the energy and particle determination. The anticoincidence shield rejects any particles leaving or entering the sides of the telescope.

Let $D_6(150)$ denote that the 150 KeV discriminator connected to detector D_6 has been triggered, while $\overline{D_6(150)}$ denotes that that discriminator has not been triggered. The obvious generalization of this notation is used

TABLE 3

PARTICLE RANGE IN TUNGSTEN ($g\ cm^{-2}$)	PROTON ENERGY (MeV)	ALPHA PARTICLE ENERGY (MeV)
0.215 - 1.07	7 - 20	28 - 80
1.07 - 4.2	20 - 45	80 - 180
4.2 - 11.15	45 - 80	180 - 320
11.15 - 25.5	80 - 130	320 - 520
25.5 - 52.5	130 - 200	520 - 800
>52.5	>200	>800

TABLE 4

DETECTOR IN WHICH THE PARTICLE STOPPED	AVERAGE ENERGY LOSS, ΔE_p, IN D_1 FOR PROTONS	AVERAGE ENERGY LOSS, ΔE_α, IN D_1 FOR ALPHAS
D_1	0 - 2.5 MeV	0 - 10 MeV
D_2	1.9 - 2.5 MeV	7.6 - 10 MeV
D_3	1.06 MeV	4.24 MeV
D_4	.58 MeV	2.32 MeV
D_5	.34 MeV	1.36 MeV
D_6	.199 MeV	0.80 MeV
D_7	.124 MeV	0.50 MeV

TABLE 5

DETECTOR	THRESHOLD (MeV)	DETECTOR	THRESHOLD (MeV)
D_1	0.100	D_3	0.150
D_1	0.420	D_4	0.050
D_1	0.750	D_4	0.220
D_1	1.250	D_5	0.150
D_1	2.300	D_6	0.150
D_2	0.050	D_7	0.100
D_2	0.200		

in the following discussion of the coincidence logic.

A proton stopping in absorber A_5 will have a kinetic energy between 130 and 200 MeV and can be distinguished by the following logic:

$$P(130\text{-}200) = D_1(100) \cdot \overline{D_1(420)} \cdot \overline{D_4(220)} \cdot D_4(050) \cdot D_6(150) \cdot \overline{D_7(100)}$$

Alpha particles stopping in A_5 with kinetic energies between 520 and 800 MeV will show:

$$\alpha(520\text{-}800) = D_1(420) \cdot D_5(150) \cdot D_6(150) \cdot D_7(100)$$

Similarly;

$$P\ (80\text{-}130) = D_1(100) \cdot \overline{D_1(420)} \cdot D_3(150) \cdot D_5(150) \cdot \overline{D_6(150)}$$

$$\alpha\ (320\text{-}520) = D_1(420) \cdot D_4(220) \cdot D_5(150) \cdot \overline{D_6(150)}$$

$$P\ (45\text{-}80) = D_1(100) \cdot \overline{D_1(750)} \cdot D_3(150) \cdot D_4(220) \cdot \overline{D_5(150)}$$

$$\alpha\ (180\text{-}320) = D_1(750) \cdot D_3(150) \cdot D_4(220) \cdot \overline{D_5(150)}$$

$$P\ (20\text{-}45) = D_1(100) \cdot \overline{D_1(1250)} \cdot D_2(200) \cdot D_3(150) \cdot \overline{D_4(220)}$$

$$\alpha\ (80\text{-}180) = D_1(1250) \cdot D_2(200) \cdot D_3(150) \cdot \overline{D_4(220)}$$

$$P\ (7\text{-}20) = D_1(420) \cdot \overline{D_1(2300)} \cdot D_2(200) \cdot \overline{D_3(150)}$$

$$\alpha\ (28\text{-}80) = D_1(2300) \cdot D_2(200) \cdot \overline{D_3(150)}$$

Protons and alphas with ranges greater than the length of the telescope are counted by requiring a coincidence between D_2, D_4, and D_7.

No separation can be made between protons with kinetic energies in excess of 200 MeV and alphas with energies above 800 MeV.

Thus:

$$P(>200),\ \alpha(>800) = D_2(050) \cdot D_4(050) \cdot D_7(100) \cdot \overline{D_2(200)}$$

The size and type of detectors were chosen on the basis of reliability over long periods of time. Depletion depth and area were kept as small as possible consistent with the minimum expected signal and the desired geometric factor. There is a 150 micron dead layer in front of D_1 and a minimum dead layer ($\sim$10 micron) between D_1 and D_2. All other detectors have relatively thick dead layers on both sides. A Lithium drift detector is used for D_7 since it requires a larger sensitive depth than the other detectors in order to get the signal for minimum ionizing protons above the noise level. D_7 has been shielded with about 53 g/cm^2 of tungsten to reduce the radiation damage.

As proton energy increases, energy loss by nuclear interaction begins to compete with ionization energy loss. If N_0 is the initial number of particles with range greater than x in the absorbing material, then N(x), the number of particles remaining after traveling a path length x, is given by the following expression:

$$N(x) = N_0\, e^{-x/\lambda},$$

where λ is the nuclear absorption length.

For tungsten, $\lambda \approx 150$ g/cm^2. Since the total thickness is about 52.9 g/cm^2, about 30 percent of the protons with energies greater than 200 MeV lose their energy by nuclear interaction with tungsten before

ELECTRON SPECTROMETER (OGO-5)

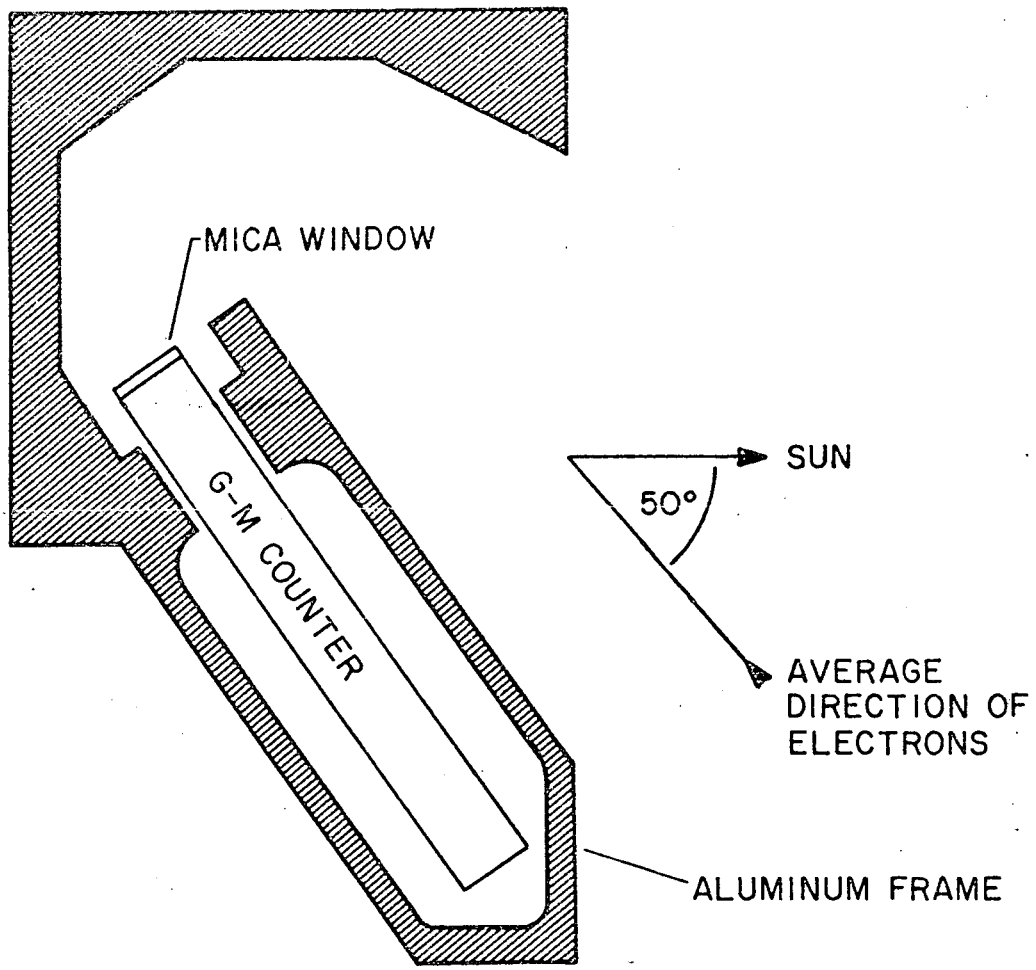

DIRECTION OF MAGNETIC FIELD PERPENDICULAR TO THE PLANE OF THE DIAGRAM

Figure 6

arriving at D7. Ten percent of the particles greater than 100 MeV are lost due to nuclear interaction before arriving at D_6.

C. Electron Spectrometer

The arrangement of the electron spectrometer is shown schematically in Figure 6. A magnetic field perpendicular to the plane of the diagram is obtained with a permanent magnet. Trajectories of the electrons entering the aperture of the spectrometer are bent by the magnetic field and then detected by a GM counter. For a given geometry, the combination of the magnetic field strength and the window transmission of the GM counter determines the range of electron energies to which the spectrometer is sensitive.

In the OGO-5 experiment two energy ranges, viz. 22-27 KeV and 50-90 KeV, are obtained by including two separate detector assemblies similar to that shown in Figure 6. The GM counters used are Lionel Type 205 HT operated at ~700 volts. In the 22-27 KeV assembly, the magnetic field is ~500 gauss and the GM counter has a 0.6 mg cm^{-2} mica window. The geometry factor is 0.1 cm^2sr. In the 50-90 KeV assembly the magnetic field is ~1000 gauss and the GM counter has a 1.4 mg cm^{-2} mica window. The geometry factor is 0.2 cm^2sr.

The directional response of the spectrometer has been determined in the laboratory with β-ray spectrum from N_i^{63} and C^{14} sources. It is found that for both the energy ranges, the average direction of detected electrons is as shown in Figure 6. Away from this direction the response falls off with FWHM of ~40°.

It should be pointed out that the spectrometer is also sensitive to X-rays which, after scattering from the aluminum frame, enter the window of the GM counter.

TABLE 6

0 0 0 0 x x x x x	=	0	+ 1	(xxxxx)
0 0 0 1 x x x x x	=	32	+ 2	(xxxxx)
0 0 1 0 x x x x x	=	96	+ 4	(xxxxx)
0 0 1 1 x x x x x	=	224	+ 8	(xxxxx)
0 1 0 0 x x x x x	=	480	+ 16	(xxxxx)
0 1 0 1 x x x x x	=	992	+ 32	(xxxxx)
0 1 1 0 x x x x x	=	2,016	+ 64	(xxxxx)
0 1 1 1 x x x x x	=	4,064	+ 128	(xxxxx)
1 0 0 0 x x x x x	=	8,160	+ 256	(xxxxx)
1 0 0 1 x x x x x	=	16,352	+ 512	(xxxxx)
1 0 1 0 x x x x x	=	32,736	+ 512	(xxxxx)
1 0 1 1 x x x x x	=	49,120	+ 512	(xxxxx)
1 1 0 0 x x x x x	=	65,504	+ 512	(xxxxx)
1 1 0 1 x x x x x	=	81,888	+ 512	(xxxxx)
1 1 1 0 x x x x x	=	98,272	+ 512	(xxxxx)
1 1 1 1 x x x x x	=	114,656	+ 512	(xxxxx)
1 1 1 1 1 1 1 1 1	=	130,528		

III. DATA HANDLING SYSTEM

The inboard electronics package contains all of the low voltage source conditioning circuitry, 10 quasi-floating point accumulators, Exp/Telemetry interference circuitry, and all readout control logic.

The low voltage source supply consists of a highly efficient switching pre-regulator followed by a chopper transformer combination. Switching of both units is synchronized with the spacecraft sync. signal. The output voltages (+3V, -6V, +12V, -18V) are used in both assemblies of the experiment. In addition, chopping signals and +15V Reg. are supplied to the High Voltage power supplies in the detector assembly.

The OGO telemetry (TM) format consists of a main frame of 128 9-bit words plus assorted sub-commutated frames. Each main frame word is read out once in 1.152 seconds when the telemetry system is in the 1 Kb/sec mode. As the maximum counting rate of the detector system was chosen to be 10^5 counts/sec, it was necessary to implement a scheme that could compress a number up to 10^5 into a 9-bit binary word with reasonable accuracy. The format used is shown in Table 6.

The four most significant bits of the TM word are assigned to the multiplier. The remaining five bits are used to convey significant figure information. The maximum error up to counts of 32,736 is 3.03 percent. At higher counts, the error becomes progressively smaller. At a count of 130,000 the error is less than 0.4 percent. A floating point accumulator (see Figure 7) is used to accomplish this compression. The operation of this accumulator is as follows. After reset, the 10 stage ring counter has a zero at the output of RC-1, the remaining nine outputs are at logical one. The zero is propagated to the left one stage for each advance pulse. When the zero reaches the tenth stage, it remains there until reset.

FLOATING POINT ACCUMULATOR (OGO-5)

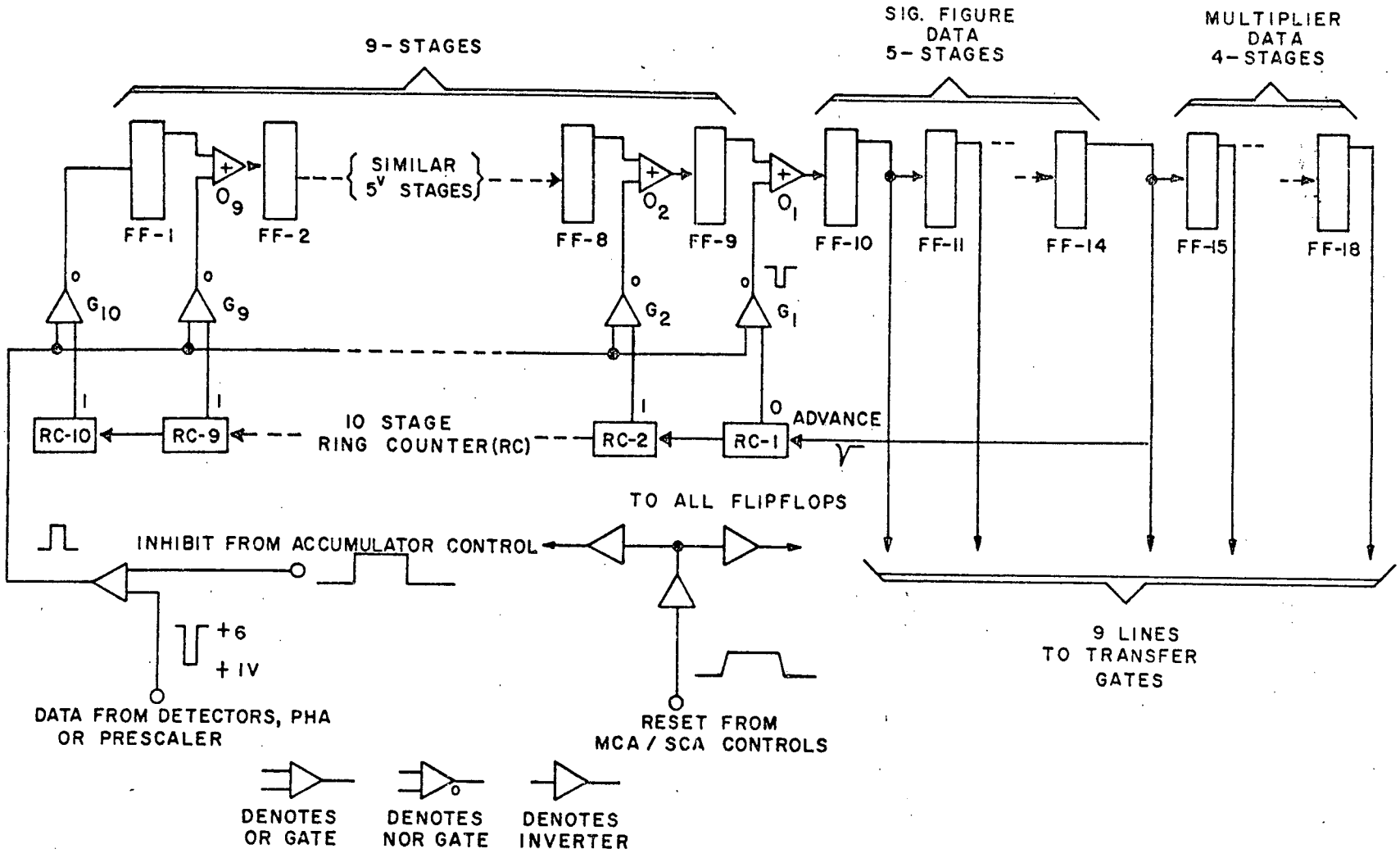

Figure 7

Input pulses are fed to ten "Nor" gates, G_1 through G_{10}. Only one of these gates is enabled at any one time. The enabled gate is determined by the location of the single zero of the ring counter. The input pulses can thus be made to appear at the output of either of G_1 through G_{10}, thus determining the injection point of the pulses into the binary counter composed of flip flops FF-1 through FF-14.

Initially after reset, the input pulses are through G_1 and O_1 into FF-10. The five flip flops FF-10 through FF-14 count input pulses in standard binary fashion up to the thirty-first pulse. Upon reception of the thirty-second pulse, FF-10 through FF-14 return to zero, sending a "one" to FF-15 and an advance pulse to the ring counter. Subsequent pulses are thus routed through G_2 and O_2 into FF-9, which prescales the input by a factor of 2. Thus 64 more input pulses are required before FF-15 is toggled and the ring counter is advanced. Subsequent input pulses are now channeled through G_3 and O_3 into FF-8; FF-8 and FF-9 now prescale the input by a factor of 4. This state continues for the next 128 pulses, whereupon the prescale factor changes to 8.

This process continues until 16,352 pulses have been accumulated. All subsequent input pulses are then routed through G_{10} and into FF-1, where they are prescaled by 512 before reaching FF-10.

The outputs of FF-10 through FF-14 contain the significant figure data, while FF-15 through FF-18 contain multiplier data. The counter accumulates precisely in accordance with the format of Table 6.

For simplicity, the accumulator was explained in terms of a ring counter; however, it is more economical, requiring less hardware, to implement the function of the ring counter with a 4-stage binary counter. The binary count can be decoded directly in the Nor gates G_1 to G_{10} by making them five input gates.

TABLE 7

OGO-E EXP 04 TELEMETRY POSITIONS

Electrons and X-rays

Energy Level	Telemetry Position
(β_1) 20-40 KeV	Subcom 69 (Main frame 97, frame 69)
(β_2) 40-80 KeV	Subcom 70 (Main frame 97, frame 70)
(X_1) 6-12 KeV	Main frame 20, frame 2, 4, 6, ..., 128
(X_2) 12-20 KeV	Main frame 19, frame 2, 4, 6, ..., 128
(X_3) 20-30 KeV	Main frame 18, frame 2, 4, 6, ..., 128
(X_4) 30-40 KeV	Main frame 17, frame 2, 4, 6, ..., 128
(X_5) 40-50 KeV	Main frame 20, frame 1, 3, 5, ..., 127
(X_6) 50-65 KeV	Main frame 19, frame 1, 3, 5, ..., 127
(X_7) 65-80 KeV	Main frame 18, frame 1, 3, 5, ..., 127
(X_8) over 80 KeV	Main frame 17, frame 1, 3, 5, ..., 127

Protons

(P_1) 7-20 MeV	Subcom 68 (Main frame 97, frame 68)
(P_2) 20-45 MeV	Main frame 25, frame 2, 10, 18, ..., 122
(P_3) 45-80 MeV	Main frame 25, frame 3, 11, 19, ..., 123
(P_4) 80-130 MeV	Main frame 25, frame 4, 12, 20, ..., 124
(P_5) 130-200 MeV	Main frame 25, frame 5, 13, 21, ..., 125
(P_6) over 200 MeV	Main frame 25, frame 6, 14, 22, ..., 126

Alphas

(α_1) 28-80 MeV	Subcom 66 (Main frame 97, frame 66)
(α_2) 80-180 MeV	Subcom 67 (Main frame 97, frame 67)
(α_3) 180-320 MeV	Main frame 25, frame 7, 15, 23, ..., 127
(α_4) 320-520 MeV	Main frame 25, frame 8, 16, 24, ..., 128
(α_5) 520-800 MeV	Main frame 25, frame 1, 9, 17, ..., 121

The counts in X_1 - X_8 should be multiplied by two (2) and the counts in P_2 - P_6, α_3 - α_5 should be multiplied by eight (8) before counting rates are calculated.

Since there are 21 sources of count data and only ten telemetry word assignments, it was necessary to commutate some of the data. The commutation scheme decided upon is as shown in Table 7. To achieve fast time resolution for solar X-rays, the PHA output is switched, four outputs at a time, into four accumulators which read out into the telemetry main frame. The remaining main frame accumulator word is commutated between 8 proton and α-particle channels. The five sub-com telemetry words are used to read the P(7-20), α(28-80), α(80-180), e^-(20-40), e^-(40-80) channels as the anticipated count rates in these channels are much lower. The two commutators are driven by a three-bit counter which is advanced with every readout of the five main frame accumulator. The three-bit counter is reset to zero during the readout of sub-com word 70.

IV. EXPERIMENT HISTORY

The OGO-5 satellite was launched on 4 March 1968 into an elliptical orbit with a period of about 62.5 hours and the perigee and apogee at a height of about 290 km and 147,000 km respectively. Initially the local time of apogee was ~0900 hours. In order to reduce the possible contribution of magnetospheric radiation to the background counting rates of the detector, the experiment is operated only at altitudes >80,000 km. Useful data are thus available for about 48 hours during each orbit. The attitude control system of the OGO-5 spacecraft failed in August 1971. Since then the operation of the OGO-5 spacecraft has been discontinued.

The solar X-ray experiment operated satisfactorily during the lifetime of the spacecraft and yielded many new and important results. Table 8 shows the background counting rates of the eight X-ray energy channels observed on 8 March 1968, 10 September 1969 and 15 July 1970. The solar

TABLE 8

OGO-5 SCINTILLATOR BACKGROUND

Channel Number	X-ray Energy (keV)	Primary Source of the Background	OBSERVED BACKGROUND (COUNTS/SEC) 8 Mar 1968 (0500-0515 UT)	10 Sept 1969 (0810-0825 UT)	15 July 1970 (0045-0100 UT)
1	9.6-19.2	Cosmic x-rays	48.4	47.5	47.7
2	19.2-32	Cosmic x-rays	16.3	16.4	17.1
3	32-48	Cosmic x-rays	9.9	10.2	9.8
4	48-64	Cosmic x-rays	5.5	5.7	5.7
5	64-80	Cosmic x-rays	3.5	3.4	3.3
6	80-104	Cosmic x-rays	3.0	2.8	2.6
7	104-128	Cosmic x-rays	1.4	1.5	1.4
8	>128	Galactic Cosmic x-rays	23.1	16.3	15.6

X-ray activity was very low at the times of these measurements. The background counting rates of the seven differential energy channels, viz. channels 1 through 7, are primarily due to the diffuse cosmic X-ray flux. Therefore these rates are expected to remain essentially constant with time unless the detector calibration changes. The background rate of the integral energy channel, viz. channel 8, is primarily due to the galactic cosmic rays and is subject to solar cycle variation even if the detector calibration remains unchanged. Table 8 shows that over a period of nearly two and one-half years there is no detectable degradation in the performance of the solar X-ray experiment.

The detector D_7 in the proton-α telescope was found to be very noisy just prior to the launch. It was therefore disabled electronically. Consequently the data for protons >200 MeV and α-particles >800 MeV are not available. The rest of the experiment performed normally.

The performance of the electron spectrometer was normal since launch until 23 September 1969. On that day the 22-27 keV channel became erratic and later stopped counting completely. The cause of this malfunction is believed to be the failure of the corresponding GM counter. The 50-90 KeV electron channel, however, continued to function normally.

V. DATA TO BE SUPPLIED TO THE NATIONAL SPACE SCIENCE DATA CENTER

The magnetic tape supplied to the National Space Sciences Data Center contains the eight 39.864-second unnormalized counting rates from the X-ray detector. A second set of tapes contain 147.456-second averages from the two electron detectors and channels 1 and 8 from the X-ray experiment. A third set of tapes contain the data from the six proton channels.

TABLE 9

BCD CARD IMAGE OF THE TAPE RECORD FORMAT

	COLUMN	FORMAT	DESCRIPTION
X-rays	1 - 3	I 3	Day
	4 - 8	I 5	Time in seconds
	9 - 17	E 9.2	Un-normalized x-ray rate (UXR) of channel 1 *
	18 - 26	E 9.2	UXR of channel 2
	.	.	.
	.	.	.
	.	.	.
	.	.	.
	72 - 80	E 9.2	UXR of channel 8
Electrons	1 - 3	I 3	Day
	4 - 8	I 5	Time in seconds
	9 - 17	E 9.2	Electrons (50-90 keV): B1
	18 - 26	E 9.2	Electrons (22-27 keV): B2
	27 - 35	E 9.2	X-rays channel 1
	36 - 44	E 9.2	X-rays channel 8
Protons	1 - 3	I 3	Day
	4 - 8	I 5	Time in seconds
	9 - 17	E 9.2	Proton channel 1 +
	17-25	E 9.2	Proton channel 2
	.	.	.
	.	.	.
	.	.	.
	.	.	.
	54 - 62	E 9.2	Proton channel 6

* X-ray channel 1 is the lowest energy channel (9.6-19.2 keV).

+ Proton channel 1 is the lowest energy channel (7-20 MeV).

The tapes were generated on CDC 6000 series equipment and are 556 cpi, 7 track, even parity (BCD) tapes. The tapes are formatted on a one file/day basis (each day's data is contained in one tape file with the files separated by a standard end of file mark). Each physical record within the file contains 37 eighty column card images for a total of 2960 BCD characters per record. Trailing blanks fill the last record of each file. A double end of file terminates the tape.

The following Tables, 9 and 10, describe the format of the logical tape record (i.e. the BCD card image) for each type of tape.

VI. MAJOR COMPUTER PROGRAMS

Figure 8 shows a schematic of the major computer programs used to process the OGO-5 experiment data. All programs were initially written for the Berkeley Campus Computer Center CDC 6400 system. They were subsequently modified for the Lawrence Berkeley Laboratory CDC 6600/7600 system and currently run there.

1. LISTER

   LISTER generates printer listings for electron and X-ray averages, produces cards containing these averages and data coverage cards which describe the bit rates and time periods covered by the input data tapes received from Goddard Space Flight Center. The program was written by G. Pitt and G. Sessler in August 1969.

2. X-RAY 24 and BETA 24

   These programs produce one inch/hour 5 cycle semi-log plots of counting rates of selected X-ray and electron channels. These plots serve as the primary display of the OGO-5 X-ray and electron data. The plots are generated on a Cal Comp 565 incremented plotter at LBL.

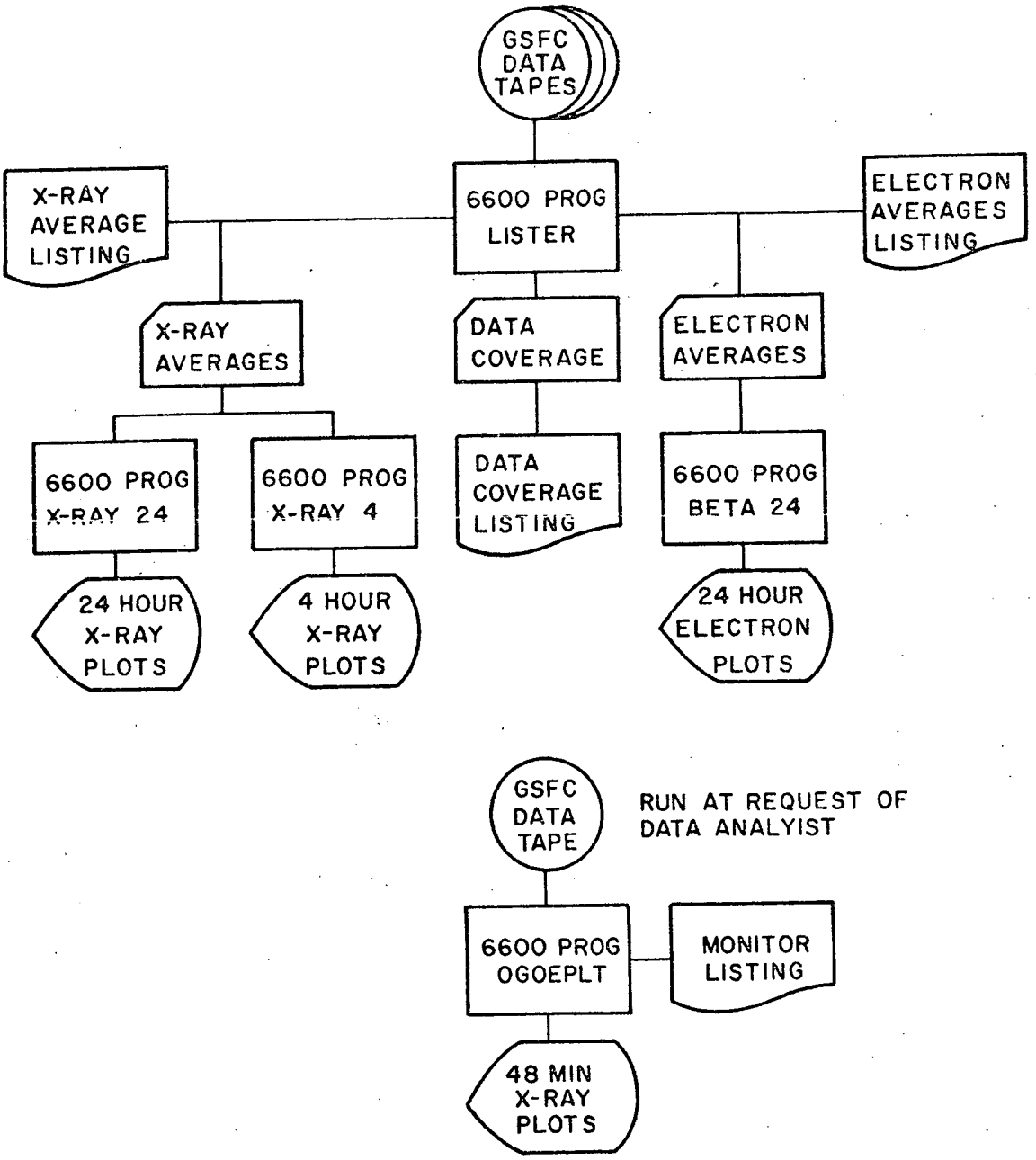
OGO-5 (E-04) DATA PROCESSING
GSFC DATA TAPES
6600 PROG LISTER
X-RAY AVERAGE LISTING
ELECTRON AVERAGES LISTING
X-RAY AVERAGES
DATA COVERAGE
ELECTRON AVERAGES
6600 PROG X-RAY 24
6600 PROG X-RAY 4
DATA COVERAGE LISTING
6600 PROG BETA 24
24 HOUR X-RAY PLOTS
4 HOUR X-RAY PLOTS
24 HOUR ELECTRON PLOTS
GSFC DATA TAPE
RUN AT REQUEST OF DATA ANALYIST
6600 PROG OGOEPLT
MONITOR LISTING
48 MIN X-RAY PLOTS

Figure 8

3. X-RAY 4 and BETA 4

   These programs generate 6 inch/hour five cycle semi-log plots for X-ray and electron averages taken over a shorter interval. Programs X-RAY 4, X-RAY 24, BETA 4 and BETA 24 were written by G. Pitt in July-August 1969.

4. OGOEPLT

   OGOEPLT produces a 2 min/inch Cal Comp plot for any number of specified time intervals of X-ray data taken from the GSFC supplied data tapes. The program is used to observe fine time structure of the experimental data. The program was written in November 1968 and revised in May 1969 by G. Pitt and G. Sessler.

VIII. BIBLIOGRAPHY OF SCIENTIFIC RESULTS

I. Publications

Anderson, K.A., Kane, S.R. and Lin, R.P., Fast electrons in solar flares, Proc. International Seminar on the Problem of Cosmic Ray Generation on the Sun, Leningrad, USSR, 1970

Kane, S.R., Observations of two components in energetic solar x-ray bursts, Ap. J. Letters 157, L139, 1969

Kane, S.R., Production of energetic x-rays during solar flares, Proc. International Symposium on Solar-Terrestrial Physics, Leningrad, USSR, 1970

Kane, S.R., An upper limit on the hardness of the non-thermal electron spectra produced during the flash phase of solar flares, Ap. J., 170, 587, 1971

Kane, S.R. and Anderson, K.A., Spectral characteristics of impulsive solar flare x-rays ≥ 10 keV, Ap. J., 162, 1003, 1970

Kane, S.R. and Donnelly, R.F., Impulsive hard x-ray and ultraviolet emission during solar flares, Ap. J., 164, 151, 1971

Kane, S.R. and Hudson, H.S., Reinterpretation of OSO-III scintillation counter measurements of hard solar x-ray spectra, Solar Phys., 14, 414, 1970

Kane, S.R., Kahler, S.W., and Kurfess, J.D., The impulsive x-ray burst of October 10, 1970, Solar Phys. (in press), 1972

Kane, S.R. and Lin, R.P., Location of the electron acceleration region in solar flares, Solar Phys., (in press), 1972

Vorpahl, J., X-radiation ($E > 10$ keV), Hα and microwave emission during the impulsive phase of solar flares, PhD Thesis, Physics Dept., University of California, Davis, August, 1971

Vorpahl, J. and Zirin, H., Identification of the hard x-ray pulse in the flare of 11-12 September 1968, Solar Phys., 11, 285, 1970

Zirin, H., Pruss, G. and Vorpahl, J., Magnetic fields, bremsstrahlung and synchrotron emission in the flare of 24 October 1969, Solar Phys., 19, 463, 1971

Vorpahl, J., X-radiation ($E > 10$ keV), Hα and microwave emission during the impulsive phase of solar flares, Solar Phys., 1972, (submitted)

II. Papers Presented at Scientific Meetings

Anderson, K.A. and Masley, A.J., Energetic solar particles, 6 to 16 July 1968, part I, AGU National Fall Meeting, San Francisco, California, December, 1969

Kane, S.R., Productions of energetic x-rays during solar flares, International Symposium on Solar-Terrestrial Physics, Leningrad, USSR, May, 1970

Kane, S.R., Characteristics of energetic electrons in the source region of impulsive solar flare x-rays, American Astronomical Society Solar Physics Meeting, Huntsville, Alabama, November, 1970

Kane, S.R., OGO-5 observations of impulsive solar flare x-rays ≥10 keV, AGU National Fall Meeting, San Francisco, California, December, 1970

Kane, S.R., Production of different non-thermal electron groups in small solar flares, Third Symposium on Ultraviolet and X-ray Spectroscopy of Astrophysical and Laboratory Plasmas, Utrecht, Netherlands, August, 1971

Kane, S.R., Relationship between solar flare x-rays and type III solar radio bursts, 136th meeting of the American Astronomical Society, San Juan, Puerto Rico, December, 1971

Kane, S.R., and Donnelly, R.F., Impulsive hard x-ray and extreme ultraviolet bursts associated with solar flares, American Astronomical Society Meeting, Boulder, Colorado, July, 1970

Kane, S. R., Lin, R. P., and Anderson, K. A., Acceleration of electrons in small solar flares, American Astronomical Society (Solar Physics Division) Meeting, College Park, Maryland, 4-6 April 1972

Lin, R.P., Kane, S.R., and Haddock, F.T., Evidence for electron excitation of Type III radio bursts, American Astronomical Society (Solar Physics Division) Meeting, College Park, Maryland, April 4 - 6, 1972.

Masley, A.J. and Anderson, K.A., Energetic solar particles, 6 to 16 July 1968, part II, AGU National Fall Meeting, San Francisco, California, December, 1969

Vorpahl, J. Various events occurring in a solar active region, American Association of Physics Teachers Annual Spring Meeting, Sacramento, California, April, 1970

Vorpahl, J., Correlation between Hα intensity and hard x-ray bursts (E ≥10 keV) in flares, American Association of Physics Teachers Meeting, Hayward, California, November, 1970

Vorpahl, J., Correlation between impulsive x-rays and Hα, American Astronomical Society Solar Physics Meeting, Huntsville, Alabama, November, 1970

Vorpahl, J., Correlation between Hα intensity and hard x-ray bursts (E ≥ 10 keV) in flares, AGU National Fall Meeting, San Francisco, California, December, 1970

II. Papers Presented at Scientific Meetings (cont.)

Vorpahl, J., X-ray (>10 keV), Hα and microwave emission during the impulsive phase of flares, 136th meeting of the American Astronomical Society, San Juan, Puerto, December, 1971

III. Seminars, Colloquiums and Informal Workshops

Kane, S.R., Two component structure of solar flare x-rays $\geq$ 10 keV, Orbiting Solar Observatories Workshop, Boulder, Colorado, August, 1969

Kane, S.R., Non-thermal x-ray emission during the flash phase of solar flares, NASA-Ames Research Center Space Sciences Seminar, August, 1970

Kane, S.R., Hard x-rays from solar flares, McDonnell-Douglas Astronautics Co. Seminar, February, 1971

Kane, S.R., Impulsive x-ray and electron emission from small solar flares, Solar Physics Workshop, Stanford University, June, 1971

Kane, S.R., Some aspects of space physics research at Berkeley, Physical Research Laboratory, Ahmedabad, India, September, 1971

Kane, S.R., Hard x-ray emission from the sun, Physical Research Laboratory, Ahmedabad, India, September, 1971

Kane, S.R., Flash phase of solar flares, Space Science and Technology Center, Thumba, India, September, 1971